ULTRA-WIDEBAND METHODS FOR UGV POSITIONING: EXPERIMENTAL AND SIMULATION RESULTS

Ka C. Cheok*, Bo Liu
Dept of Electrical& Computer Engineering, Oakland University
Rochester, MI 48309

G. R. Hudas, J. L. Overholt, M. Skalny
U.S. Army RDECOM-TARDEC
Warren, MI 48397-5000

G. E. Smid
JADI Inc.
Troy, MI, 48098

ABSTRACT

U.S. Army RDECOM-TARDEC, in collaboration with Oakland University and JADI Inc., is currently conducting novel research devoted to obtain fine-grain (centimeter accuracy) indoor positioning for unmanned ground vehicle (UGV) navigation applications using Ultra-Wideband (UWB) technologies. This paper will present recent results from advanced closed-form solutions and analyses for positioning errors, and compare them to experimental results and Cramer-Rao bounds. Agreement among the calculated and experiment standard deviations confirms validity of the techniques and lays a basis for tuning and optimizing solutions for estimating positions of unmanned ground vehicles.

1. INTRODUCTION

Within the context of conducting the basic task of navigating autonomously from point A to B, an unmanned ground vehicle (UGV) system must have sufficient knowledge of the environment, and the abilities to navigate anywhere and compute its position and orientation. These UGV capabilities can be summarized into three questions: "Where am I?", "Where am I going?", and "How do I get there?". The following paper is concerned primarily with answering the first question with a general technique known as *positioning* or *localization*.

Positioning technology is an essential feature for the navigation and guidance of a UGV. Traditional categorizations of positioning are: Standalone (dead reckoning or use of landmark recognition), satellite-base Global Positioning Systems (GPS), and terrestrial-radio-based systems (Long Range Navigation "C" configurations, etc.). Depending on the requirements, conditions, and resources in an application, positioning can employ a combination of these. However, there exist many navigation and guidance challenges which include precision issues, fast positioning needs, loss of signal due to environment, etc., especially in indoor environments involving non-line-of-sight conditions.

Recent growth of interest in pervasive computing and location aware systems provides a strong motivation to develop the techniques for estimating the location of UGVs in both outdoor and indoor environments. There have been many approaches to solve this problem including TOA (Time Of Arrival), TDOA (Time Difference Of Arrival), and ROA (Received signal strength Of Arrival) which are location aware methods that calculate the relative distance between reference nodes and a sensor (UGV) node (Patwari et al., 2003; Wang et al., 2003; Lee et al., 2005). TOA uses the time of received signals from the reference nodes to calculate distance. This method requires accurate time synchronization among all of the sensor nodes and reference nodes. In the case of TDOA, synchronized reference nodes receive signals from a sensor node and calculate time differences between times on which each reference node received signals from the sensor node. These techniques provide robustness and precision in ranging and identification of the transmission source in a single operation. Advanced systems solution methods can be used to compute the position of an object (in this case a UGV) based on the TOAs and TDOAs. Uniqueness of this system is the ability to integrate UWB/RAC electronics with TOA/TDOA solutions (Cheok et al., 2004).

Analysis techniques involving the Cramer-Rao bound (CRB) provide methods for calculating a lower bound on the covariance of any unbiased positioning estimator which uses connectivity, TOA, and TDOA measurements (Patwari et. al, 2005; Chang et al., 2006; Rydstrom et al. 2006). This lower bound is useful for determining the

Report Documentation Page

Form Approved
OMB No. 0704-0188

1. REPORT DATE	2. REPORT TYPE	3. DATES COVERED
01 NOV 2006	**N/A**	**-**

4. TITLE AND SUBTITLE	5a. CONTRACT NUMBER
Ultra-Wideband Methods For Ugv Positioning: Experimental And Simulation Results	5b. GRANT NUMBER
	5c. PROGRAM ELEMENT NUMBER
6. AUTHOR(S)	5d. PROJECT NUMBER
	5e. TASK NUMBER
	5f. WORK UNIT NUMBER
7. PERFORMING ORGANIZATION NAME(S) AND ADDRESS(ES) **Dept of Electrical& Computer Engineering, Oakland University Rochester, MI 48309**	8. PERFORMING ORGANIZATION REPORT NUMBER
9. SPONSORING/MONITORING AGENCY NAME(S) AND ADDRESS(ES)	10. SPONSOR/MONITOR'S ACRONYM(S)
	11. SPONSOR/MONITOR'S REPORT NUMBER(S)

12. DISTRIBUTION/AVAILABILITY STATEMENT
Approved for public release, distribution unlimited

13. SUPPLEMENTARY NOTES
See also ADM002075., The original document contains color images.

14. ABSTRACT

15. SUBJECT TERMS

16. SECURITY CLASSIFICATION OF:			17. LIMITATION OF ABSTRACT	18. NUMBER OF PAGES	19a. NAME OF RESPONSIBLE PERSON
a. REPORT	b. ABSTRACT	c. THIS PAGE			
unclassified	**unclassified**	**unclassified**	**UU**	**7**	

Standard Form 298 (Rev. 8-98)
Prescribed by ANSI Std Z39-18

'best-case' positioning algorithm. The CRB on estimator covariance is a function of: the number of unknown/known location nodes; sensor geometry; dimensionality; measurement/computation type (TOA, TDOA, etc.); channel parameters; and, node connectivity.

A UWB Location Positioning System (LPS) has been set up for navigating and guidance of UGVs with the main objectives of analyzing and validating accuracies of the UWB LPS in locating position. This paper not only addresses the problem of time-based positioning using a derived closed form solution, but also the characterization of uncertainty to determine the quality of solution in both theory and experimental results.

2. EXPERIMENTS

2.1 Experimental Setup

Figure 1 shows a MSSI Sapphire Precision Asset Location System (PALS) that uses UWB technology to RFID and locate the position of tagged assets. A typical PALS consists of a central processing station (CPS), four

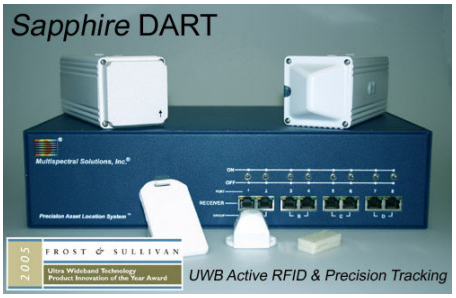

Figure 1: Multispectral Solutions Inc. (MSSI) Sapphire Precision Asset Location System (PALS).

receivers, a reference transmitter tag and multiple asset transmitter tags. The receivers are positioned at known locations and cable linked directly to the CPS. The transmitter tags used in the experiment are 1"x1"x1/2" in size, have a range in excess of 650 ft, and update at a rate of 1, 15 or 60 samples/sec. The tags transmit sub-nanosecond pulse technology that can penetrate through multiple obstructions in indoor and outdoor environments. A reference transmitter tag is required to synchronize the clocks in the receivers. The receivers receive RFID transmissions from asset tags and feed the time of arrivals (TOA) to CPS. Location of each asset tag is then computed by the CPS. The PALS claims to be capable of precision tracking accuracy and resolution better than 4". Figure 2 depicts a bird's eye view of the experimental test site (Shotwell-Gustafson Pavilion at the Oakland University SmartZone) and the layout of the

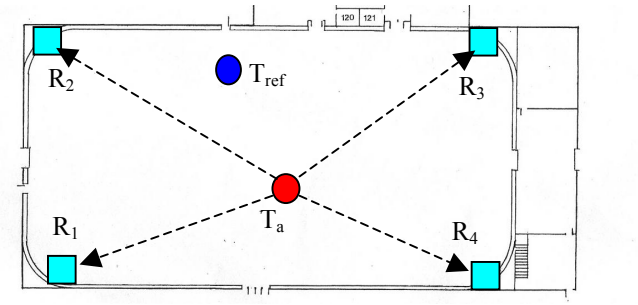

Figure 2: Experimental Setup.

UWB PALS receivers in the Pavilion. Four receivers were mounted at (units in feet):

$$\left\{\begin{bmatrix} x \\ y \\ z \end{bmatrix}_{R_j}\right\} = \begin{bmatrix} 15.710 & 1.480 & 200.850 & 201.57 \\ 0.500 & 102.810 & 102.760 & 0.4583 \\ 11.500 & 11.720 & 14.490 & 13.430 \end{bmatrix} \quad (1)$$

The reference tag T_{ref}, fixed at a known location, is used to synchronize the clocks in receivers R_j. Let t_i denote the time-of-arrival (TOA) of the transmission from the object or asset attached tag T_a at each R_j using the synchronized clocks. Assume that the clock measurements $t_i + \Delta t_i$, where Δt_i denotes errors, have statistical properties $\mathrm{E}(\Delta t_i) = 0$ and $\mathrm{E}(\Delta t_i^2) = \sigma_T^2$. σ_T is the error variance in measurement of t_i and represent the range resolution of the UWB LPS. The LPS specifies that $\sigma_T \approx 0.3 \times 10^{-9}$ sec. If v_p is the propagation speed ($v_p = 0.98357 \times 10^9$ fps) of electromagnetic wave, then the uncertain measurement errors in distance or range are given by $v_p \sigma_T$.

In the above setup, the receivers were mounted at approximately the same height (nearly coplanar). This allows us to simplify and perform a 2-D positioning analysis and testing of the setup. Let the 2-D location of each receiver be denoted by,

$$\mathbf{p}_j = \begin{bmatrix} x_j \\ y_j \end{bmatrix}, \quad j = 1, 2, 3, 4, \quad (2)$$

and that of the asset or sensor tag be,

$$\mathbf{p}_a = \begin{bmatrix} x \\ y \end{bmatrix}_a . \quad (3)$$

The UWB PALS measures the distance r_i by clocking the time-of-arrivals. The distance relationship between the tag and receiver j is:

$$r_i = \sqrt{(x_a - x_i)^2 + (y_a - y_i)^2} \tag{4}$$

2.2 Problem Statement

Now, suppose that the location of the sensor is calculated by an (any) estimator as $\begin{bmatrix} \hat{x}_a & \hat{y}_a \end{bmatrix}^T$. Let σ_a^2 be defined as the location variance of the estimator as:

$$\sigma_a^2 \triangleq \text{var}(\hat{x}_a) + \text{var}(\hat{y}_a) = \text{E}(\hat{x}_a^2) + \text{E}(\hat{y}_a^2) \tag{5}$$

and σ_a being the standard deviation. The following section of this paper will compare the standard deviations using variances computed from the Cramer-Rao Bound (CRB), TOA method, and the TDOA method all of which were obtained from experimental tests from the SmartZone Test setup.

3. RESULTS

3.1 Cramer-Rao Bound (CRB)

Let H denote the communication status between Sensor a and the receivers. E.g., $H = \{1,\ 2,\ 3,\ 4\}$ if Sensor a makes measurements with receivers 1, 2, 3 & 4; and $H = \{1,\ 2,\ 4\}$ if only with receivers 1, 2 and 4. A *Fisher Information Matrix (FIM)* is formed as follows:

$$\mathbf{F} = \begin{bmatrix} F_{xx} & F_{xy} \\ F_{xy} & F_{yy} \end{bmatrix} \tag{6}$$

where,

$$\begin{aligned} F_{xx} &= \gamma \sum_{i \in H} (x_a - x_i)^2 / r_i^2 \\ F_{xy} &= \gamma \sum_{i \in H} (x_a - x_i)(y_a - y_i) / r_i^2 \\ F_{yy} &= \gamma \sum_{i \in H} (y_a - y_i)^2 / r_i^2 \end{aligned} \tag{7}$$

For TOA analyses, the channel constant term γ is defined as $\gamma = \dfrac{1}{\left(v_p \sigma_T\right)^2}$. The CRB matrix is the inverse of FIM and given by,

$$\mathbf{Q}_{CRB} = \begin{bmatrix} q_{xx} & q_{xy} \\ q_{xy} & q_{yy} \end{bmatrix}_{CRB} = \left[\mathbf{F}\right]^{-1}. \tag{8}$$

The diagonal elements of $\mathbf{Q}_{CRB}$ are the variance bound for estimation of sensor a location. The CRB asserts that,

$$\sigma_a^2 \ \geq \ \sigma_{CRB}^2 = q_{xx,CRB} + q_{yy,CRB} \tag{9}$$

Figure 3 shows an application of CRB to the UWB LPS over the Test Setup. The analysis assumes that the asset

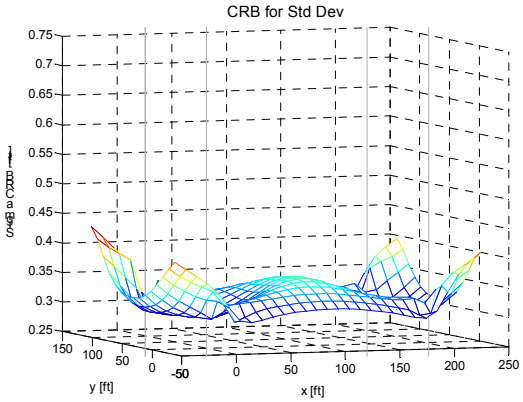

Figure 3: Example of CRB to the UWB LPS from the experimental setup.

tag (Sensor a) communicates with all the receivers, thus $H = \{1,\ 2,\ 3,\ 4\}$.

The CRB reveals the best possible standard deviation σ_a that can be achieved in estimating the location of Sensor a based on the measurement configuration.

3.2 Time-Of-Arrival (TOA) Method

The TOA method calculates location $\mathbf{p}_a = \begin{bmatrix} x_a & y_a \end{bmatrix}^T$ based on knowing the range measurements r_i. Manipulating the relationship,

$$r_i^2 = (x_a - x_i)^2 + (y_a - y_i)^2, \ i = 1, \ldots, 4 \tag{10}$$

yields x & y as,

$$\begin{bmatrix} x \\ y \end{bmatrix}_{TOA} = \frac{1}{2}\left[\mathbf{A}_{TOA}\right]^{\#} \begin{bmatrix} h_2^2 - h_1^2 - (r_2^2 - r_1^2) \\ h_3^2 - h_2^2 - (r_3^2 - r_2^2) \\ h_4^2 - h_3^2 - (r_4^2 - r_3^2) \\ h_1^2 - h_4^2 - (r_1^2 - r_4^2) \end{bmatrix} \tag{11}$$

where,

$\mathbf{A}_{TOA} = \begin{bmatrix} x_{2,1} & y_{2,1} \\ x_{3,2} & y_{3,2} \\ x_{4,3} & y_{4,3} \\ x_{1,4} & y_{1,4} \end{bmatrix}$, $[\ ]^{\#}$ denotes the generalized inverse matrix operation, and $h_i^2 \triangleq x_i^2 + y_i^2$, $x_{i,j} \triangleq x_i - x_j$ & $y_{i,j} \triangleq y_i - y_j$.

A TOA measurement with error can be expressed as,

$$r_i + \eta_{r_i} = v_p \left(t_i + \eta_{t_i} \right) \tag{12}$$

where $t_i + \eta_{t_i}$ is the time of arrival with time errors. In the TOA case, $\eta_{r_i} = v_p \eta_{t_i}$ and $\mathrm{E}(\eta_{r_i}^2) = \sigma_{r_i}^2 = \left(v_p \sigma_T \right)^2$. The TOA measurements inject errors in the calculations as follows:

$$\begin{bmatrix} x + \Delta x \\ y + \Delta y \end{bmatrix}_{TOA} = \frac{1}{2} \mathbf{A}_{TOA}^{\#} \begin{bmatrix} h_2^2 - h_1^2 - \left((r_2 + \eta_{r_2})^2 - (r_1 + \eta_{r_1})^2 \right) \\ h_3^2 - h_2^2 - \left((r_3 + \eta_{r_3})^2 - (r_2 + \eta_{r_2})^2 \right) \\ h_4^2 - h_3^2 - \left((r_4 + \eta_{r_4})^2 - (r_3 + \eta_{r_3})^2 \right) \\ h_1^2 - h_4^2 - \left((r_1 + \eta_{r_1})^2 - (r_4 + \eta_{r_4})^2 \right) \end{bmatrix} \tag{13}$$

It can be shown that

$$\begin{bmatrix} \Delta x \\ \Delta y \end{bmatrix}_{TOA} \approx -\mathbf{A}_{TOA}^{\#} \begin{bmatrix} r_2 \eta_{r_2} - r_1 \eta_{r_1} \\ r_3 \eta_{r_3} - r_2 \eta_{r_2} \\ r_4 \eta_{r_4} - r_3 \eta_{r_3} \\ r_1 \eta_{r_1} - r_4 \eta_{r_4} \end{bmatrix} \tag{14}$$

where we apply the fact that $r_i \gg \eta_{r_i}$ in the last expression. It follows that the variance of estimation using TOA method is given by,

$$\begin{bmatrix} q_{xx} & q_{xy} \\ q_{xy} & q_{yy} \end{bmatrix}_{TOA} = E \begin{bmatrix} (\Delta x)^2 & \Delta x \Delta y \\ \Delta y \Delta x & (\Delta y)^2 \end{bmatrix}_{TOA}$$

$$\approx \mathbf{A}_{TOA}^{\#} \begin{bmatrix} r_2^2 \sigma_{r_2}^2 + r_1^2 \sigma_{r_1}^2 & -r_2^2 \sigma_{r_2}^2 & 0 & -r_1^2 \sigma_{r_1}^2 \\ -r_2^2 \sigma_{r_2}^2 & r_3^2 \sigma_{r_3}^2 + r_2^2 \sigma_{r_2}^2 & -r_3^2 \sigma_{r_3}^2 & 0 \\ 0 & -r_3^2 \sigma_{r_3}^2 & r_4^2 \sigma_{r_4}^2 + r_3^2 \sigma_{r_3}^2 & -r_4^2 \sigma_{r_4}^2 \\ -r_1^2 \sigma_{r_1}^2 & 0 & -r_4^2 \sigma_{r_4}^2 & r_1^2 \sigma_{r_1}^2 + r_4^2 \sigma_{r_4}^2 \end{bmatrix} \mathbf{A}_{TOA}^{\#T} \tag{15}$$

A combined measure of the variance of the TOA computed location $\mathbf{p}_{TOA} = \begin{bmatrix} x & y \end{bmatrix}_{TOA}^T$ can be expressed as

$$\sigma_{TOA}^2 = q_{xx,TOA} + q_{yy,TOA}. \tag{16}$$

Figure 4 illustrates standard deviation σ_{TOA} for the experimental UWB LPS.

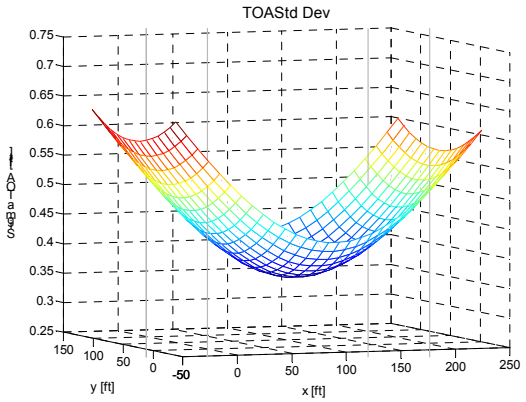

Figure 4: TOA standard deviation for the experimental UWB LPS.

3.3 Time-Difference-Of-Arrival (TDOA)

The TDOA method calculates the location $\mathbf{p}_a = \begin{bmatrix} x_a & y_a \end{bmatrix}^T$ using the difference in distances

$$r_{i,1} \triangleq r_i - r_1 = v_p \left(t_i - t_1 \right), \quad i = 2,3,4 \tag{17}$$

where $r_{i,1}$ can be computed from TDOA $\left(t_i - t_1 \right)$. It can be shown that,

$$\begin{aligned} r_{i,1}^2 + 2 r_{i,1} r_1 &= r_i^2 - r_1^2 \\ &\triangleq h_i^2 - h_1^2 - 2 x_{i,1} x - 2 y_{i,1} y \end{aligned} \tag{18}$$

which leads to the closed-form TDOA relationship,

$$\begin{bmatrix} x \\ y \\ r_1 \end{bmatrix}_{TDOA} = \frac{1}{2} \mathbf{A}_{TDOA}^{\#} \begin{bmatrix} h_2^2 - h_1^2 - r_{2,1}^2 \\ h_3^2 - h_1^2 - r_{3,1}^2 \\ h_4^2 - h_1^2 - r_{4,1}^2 \end{bmatrix} \tag{19}$$

where $\mathbf{A}_{TDOA} = \begin{bmatrix} x_{2,1} & y_{2,1} & r_{2,1} \\ x_{3,1} & y_{3,1} & r_{3,1} \\ x_{4,1} & y_{4,1} & r_{4,1} \end{bmatrix}$.

Now, denote $r_{i,1} + n_{r_{i,1}}$ as the measurement of $r_{i,1}$ with timing error $n_{r_{i,1}} = v_p \left(\Delta t_i - \Delta t_1 \right)$. Note that in the TDOA

case, $\sigma^2_{r_{i,1}} = \mathrm{E}(n^2_{r_{i,1}}) = 2\sigma^2_T$. Introduce the measurements in the TDOA relationship as follows:

$$\begin{bmatrix} x_{2,1} & y_{2,1} & r_{2,1}+\eta_{r_{2,1}} \\ x_{3,1} & y_{3,1} & r_{3,1}+\eta_{r_{3,1}} \\ x_{4,1} & y_{4,1} & r_{4,1}+\eta_{r_{4,1}} \end{bmatrix} \begin{bmatrix} x+\Delta x \\ y+\Delta y \\ r_1+\Delta r_1 \end{bmatrix}_{TDOA} = \frac{1}{2}\begin{bmatrix} h_2^2-h_1^2-(r_{2,1}+\eta_{r_{2,1}})^2 \\ h_3^2-h_1^2-(r_{3,1}+\eta_{r_{3,1}})^2 \\ h_4^2-h_1^2-(r_{4,1}+\eta_{r_{4,1}})^2 \end{bmatrix} \quad (20)$$

It can be shown in practice that the conditions where $\eta_{r_{i,1}} \ll r_{i,1}$ and $\Delta r_1 \ll r_1$ are often true. Then it follows that,

$$\begin{bmatrix} \Delta x \\ \Delta y \\ \Delta r_1 \end{bmatrix}_{TDOA} \approx -\mathbf{A}^{\#}_{TDOA} \begin{bmatrix} r_2\,\eta_{r_{2,1}} \\ r_3\,\eta_{r_{3,1}} \\ r_4\,\eta_{r_{4,1}} \end{bmatrix} \quad (21)$$

The variance of the errors in the TDOA computation is given by,

$$\begin{bmatrix} q_{xx} & q_{xy} & q_{xr_1} \\ q_{xy} & q_{yy} & q_{yr_1} \\ q_{xr_1} & q_{yr_1} & q_{r_1r_1} \end{bmatrix}_{TDOA} \triangleq \mathrm{E}\left[\begin{bmatrix} \Delta x \\ \Delta y \\ \Delta r_1 \end{bmatrix}\begin{bmatrix} \Delta x \\ \Delta y \\ \Delta r_1 \end{bmatrix}^T\right] = \mathbf{A}^{-1}_{TDOA}\begin{bmatrix} r_2^2\,\sigma^2_{r_{2,1}} & 0 & 0 \\ 0 & r_3^2\,\sigma^2_{r_{3,1}} & 0 \\ 0 & 0 & r_4^2\,\sigma^2_{r_{4,1}} \end{bmatrix}\left(\mathbf{A}^{-1}_{TDOA}\right)^T \quad (22)$$

where $\sigma^2_{r_{i,1}} = 2\sigma^2_T$ as noted earlier. A combined measure of the variance of the TDOA computed location $\mathbf{p}_{TDOA} = \begin{bmatrix} x & y \end{bmatrix}^T_{TDOA}$ can be expressed as,

$$\sigma^2_{TDOA} = q_{xx,TDOA} + q_{yy,TDOA} \quad (23)$$

The standard deviation σ_{TDOA} for the experimental UWB LPS was computed for grid points over the Pavilion, and plotted in Figure 5.

It is seen that σ_{TDOA} becomes excessively large at certain locations. This is due to $\mathbf{A}_{TDOA}$ being ill-conditioned at those locations. The situation can be minimized by re-configuring the locations of the receivers. Alternatively, one can formulate additional

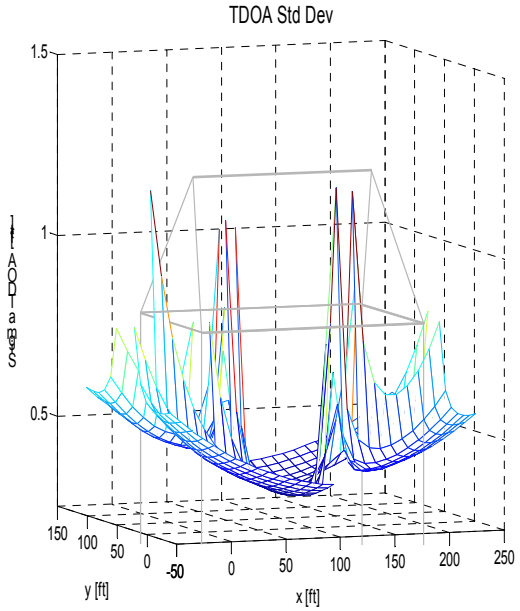

Figure 5: TDOA standard deviation for the experimental UWB LPS.

relationships to supplement the information for the TDOA relationships. Work on configuring TDOA parameters to maximize their performance is underway and will be reported elsewhere.

3.4 Experimental Results

Experiments were conducted to measure and compute the statistical variance of the MSSI PALS. A

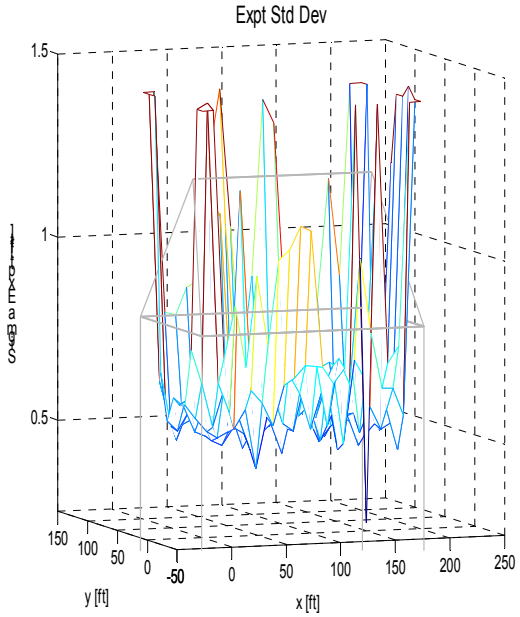

Figure 6: Actual standard deviations from the UWB PALS.

total of 231 sets of experimental data were collected with sensors statically placed over evenly spaced 11 x 21 grids in the Pavilion. Each set of experiment data consists of approximate 500 readings of the location [x y z]' of the sensor at a particular location. The statistical mean and variance were then computed. Figure 6 shows the standard deviations obtained from the experiments. It is noted that the general distribution property of standard deviations from the experimental data resembles that of the TDOA. This indeed should be the case since the MSSI PALS employs a TDOA technique to generate a location estimate.

3.5 Comparison of Results

Figure 7 superposes and compares the standard deviations computed from the CRB, TOA and TDOA techniques and the experimental data. Observe that the

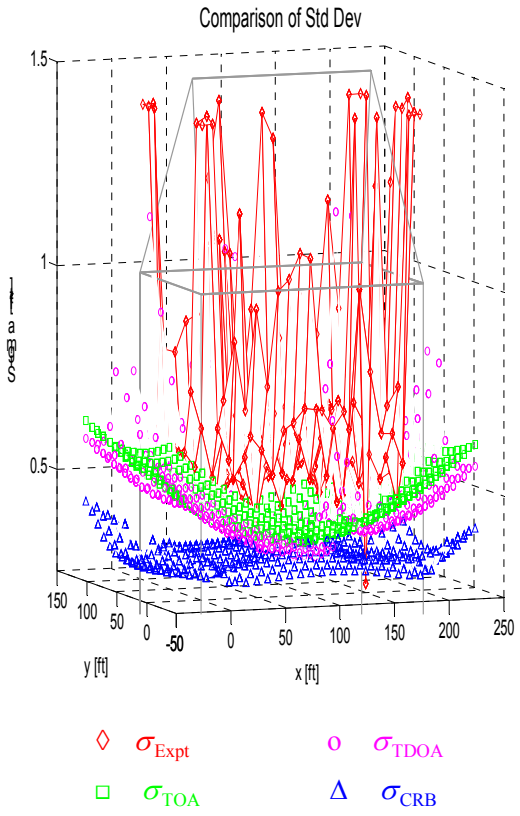

Figure 7: Comparison of standard deviations from experiment data,. TDOA, TOA and CRB calculations.

CRB really is lower bound for the other standard deviations. The TOA and TDOA deviations are very close to one another, except that TDOA deviations deteriorate at ill-conditioned locations. The experimental standard deviations are larger than all the other deviations. This can be expected since many additional factors contribute to measurements errors in practice. Overall, the CRB calculation is verified with results from the TOA, TDOA and experimental analysis.

The CRB, TOA and TDOA calculations were based on parameters provided by the manufacturer, and on physical layout of the receivers. In practice, the experimental results can be used as reference data for adjusting the parameters for the system.

4. CONCLUSION AND FUTURE WORK

The results shown in Figure 7 provide a significant opportunity for performance improvement involving the navigation of autonomous systems. Since these systems rely heavily on their ability to acquire their accurate position, the improvement in this ability will result in superior results for the waypoint-following and target tracking.

The Cramer-Rao Bound provides for a technique to predict a *lower bound* for the standard deviation of the TOA or TDOA position calculation using UWB range measurements. These predictions can be used to evaluate the quality of position calculations for a series of combinations of range measurements. In other words, with the CRB, the navigation system is now able to evaluate the 'quality' of a combination of range measurements, and to decide which combination is best to use for the calculation of the vehicle's position.

The experimental data validates the analyses for CRB, TOA and TDOA, in that it envelopes or form an *upper bound* for calculated the standard deviations. The theoretical analyses, verified by practical experiments, can therefore be applied to other algorithms with confidence. This is also an important contribution of the paper.

For military applications, unmanned systems technology with accurate positioning can greatly benefit the soldiers/operators by reducing dangerous tasks to robotic operations, therefore potentially preventing harm and saving the lives of soldiers. One such application is for anti-personnel mine detection, using the Future Combat System (FCS) Small Unmanned Ground Vehicle (SUGV) system. Such an application requires high-precision navigation technology to conduct accurate sweeps. We feel that our proposed RF navigation system can provide a potential solution for path planning, mobility, and control algorithm development.

Future work will involve further analysis of the matrices to include eigen-structure analysis for determining conditioning of the matrices. This will assist

in understanding the measurements as well as provide potential strategies of where to place the receivers.

5. ACKNOWLEDGEMENT

The authors would like to thank Michel Franken, Nithin Chandrababu and Pavan Vempaty for conducting experiments with the UWB PALS. The authors would also like to acknowledge the assistance of Multispectral Solutions, Inc. (http://www.multispectral.com).

6. REFERENCES

Chang, C., Sahai, A., 2006: Cramer-Rao-Type Bounds for Localization. *EURASIP J. on Applied Signal Processing*, **2006**, Article 94287, 13 pgs.

Cheok, Ka. C., Hudas, G., Overholt, J.L., Smid, E., 2004: Ultra-Wideband RF Methods for Localizing an Autonomous Mobile Robot. Proceedings, *24th Army Science Conference*, Orlando, Fl.

Lee, Y., Kwon, E., Lim, J., 2005: Self Location Estimation Scheme Using ROA in Wireless Sensor Networks. Proceedings, *Intl. Workshop on RFID and Ubiquitous Sensor Networks*, Nagasaki, Japan, 1169-1177.

Patwari, N., Hero, A., Perkins, M., Correal, N., O'Dea, B., 2003: Relative Location Estimation in Wireless Sensor Networks. *IEEE Trans. on Signal Processing*, **51**, 2137-2148.

Patwari, N., Ash, J., Kyperountas, A., Hero, O., Moses, R.M., Correal, N., 2005: Locating the Nodes: Cooperative Localization in Wireless Sensor Networks. *IEEE Signal Processing Magazine*, **22**, 54-69.

Rydstrom, M., Urruela, A., Strom, E., Svensson, A., 2006: Autonomous Positioning Techniques Based on Cramer-Rao Lower Bound Analysis. *J. on Applied Signal Processing*, **2006**, Article 93043, 10 pgs.

Wang, X., Wang, Z., O'Dea, B., 2003: A TOA-Based Location Algorithm Reducing the Errors Due to Non-Line-of-Sight (NLOS) Propagation. *IEEE Trans. on Vehicular Technology*, **52**, 112-116.